

Theoretical molecular structure and experimental dipole moment of *cis*-1-chloro-2-fluoroethylene

Alberto Gambi,^{*a} Gabriele Cazzoli,^b Luca Dore,^b Andrea Mazzavillani,^b Cristina Puzzarini,^c Paolo Palmieri^c and Alessandro Balzan^d

^a Dipartimento di Scienze e Tecnologie Chimiche, Via Cotonificio 108, I-33100 Udine, Italy.

E-mail: gambi@uniud.it; Fax: +39 0432 558803; Tel: +39 0432 558856

^b Dipartimento di Chimica "G. Ciamician", Via Selmi 2, I-40126 Bologna, Italy

^c Dipartimento di Chimica Fisica ed Inorganica, Viale Risorgimento 4, I-40136 Bologna, Italy

^d Dipartimento di Chimica Fisica, D. D. 2137, I-30123 Venezia, Italy

Received 23rd December 1999, Accepted 23rd February 2000

The equilibrium geometry of *cis*-1-chloro-2-fluoroethylene has been evaluated using two different *ab initio* methods: the coupled-cluster (CC) approach and Møller–Plesset perturbation theory. Accurate predictions have been obtained. Using both methods, the dipole moment has been estimated numerically as energy derivative with respect to an applied electric field at zero field strength. The experimental dipole moment of *cis*-1-chloro-2-fluoroethylene has been determined by observing the Stark spectrum of the $J = 4_{0,4} \leftarrow 3_{1,3}$ and $J = 4_{1,3} \leftarrow 4_{0,4}$ transitions. The spectrum profile has been fitted to a model function computed as a sum of Lorentzian profiles over the hyperfine-Stark components, whose frequencies have been derived by diagonalizing the full rotational–quadrupole-Stark Hamiltonian matrix for each value of the applied electric field. Very good agreement between experimental and theoretical dipole moment has been obtained.

1 Introduction

Earlier studies of the microwave spectra of *cis*-1-chloro-2-fluoroethylene were carried out by Howe,¹ who obtained the ground state rotational constants and chlorine nuclear quadrupole coupling constants. They were limited to relatively low J transitions in the 15–25 GHz region. Recently, the millimeter-wave spectra of this molecule have been recorded up to 245 GHz and a set of ground state molecular constants including sextic centrifugal distortion terms has been obtained for both isotopomers (in natural abundance) $\text{CH}^{35}\text{Cl}=\text{CHF}$ and $\text{CH}^{37}\text{Cl}=\text{CHF}$.²

Low-resolution infrared studies on the *cis*- $\text{CHCl}=\text{CHF}$ molecule were also performed a long time ago,³ and established the vibrational assignment of fundamentals, overtones and combination bands.

In recent years, halogenated ethylenes have become the subject of spectroscopic studies due to their significant role as air pollutants. These compounds are reactive molecules and the most important transformation processes involve photolysis and chemical reactions with atmospheric ozone and hydroxyl radicals.^{4,5}

Using this perspective, the high-resolution infrared spectra of the ν_6 fundamental mode have been recorded with a diode laser spectrometer and molecular constants for the excited vibrational state have been determined.⁶

To our knowledge, no dipole moment and accurate structure have up to now been obtained either experimentally or theoretically for *cis*-1-chloro-2-fluoroethylene. These data are of considerable interest in fully characterizing the spectroscopic properties of this molecule, especially for intensities measurements and modelling as atmospheric pollutant.

This work deals with the equilibrium geometry of *cis*-1-chloro-2-fluoroethylene evaluated using *ab initio* methods at high level of theory and with the experimental dipole moment determined from measurements of the Stark spectra of selec-

ted rotational transitions. Finally, the dipole moment has been calculated using different *ab initio* methods and compared to the experimental value.

2 Molecular structure

2.1 Computational details

Since for this molecule the Hartree–Fock (HF) determinant strongly dominates the electronic molecular wavefunction, accurate predictions have been given by coupled cluster theory with single and double excitations (CCSD) including the effects of connected triple substitutions, which usually determine the most important higher contributions, by means of perturbation theory. Since full inclusion is rather expensive, we have used CCSD(T) method,^{7–9} which is a good approximation to take into account triple excitations. Fourth order Møller–Plesset manybody perturbation theory (MP4),^{7,10} including single, double, triple and quadruple substitutions from the HF configuration, has also been employed and gives very close estimates of the equilibrium geometry and molecular dipole moment.

In the equilibrium structure calculations the correlation consistent double-zeta (cc-pVDZ) and triple-zeta (cc-pVTZ) basis sets¹¹ have been used, which comprise 70 and 152 contracted Gaussian-type orbitals (cGTOs), respectively. Since the cc-pVTZ gives better results with slight increasing of computational effort, this basis set (s, p, d, f functions for C, F and Cl atoms; s, p, d for H atoms) has been employed in the final equilibrium geometry optimization and in the following dipole moment computations. Unfortunately, we were not able to use the cc-pVQZ basis set,¹¹ which has been found to be too big; but, as highlighted in ref. 12, for most methods and applications the cc-pVTZ basis provides results sufficiently close to the basis set limit.

Table 1 Computed equilibrium geometry of *cis*-1-chloro-2-fluoroethylene (distances in Å and angles in degrees)

	MP4/VTZ	CCSD(T)/VTZ	Ref. 1 ^a	Ref. 18 ^b
C(1)–Cl	1.726	1.726	1.726	1.724
C(1)–H	1.079	1.078	1.079	1.072
C(1)–C(2)	1.333	1.332	1.333	1.309
C(2)–F	1.337	1.334	1.348	1.318
C(2)–H	1.081	1.081	1.079	1.072
∠ ClC(1)C(2)	123.31	123.31	123.6	123.68
∠ HC(1)C(2)	120.30	120.39	123.2	120.88
∠ FC(2)C(1)	123.05	123.05	121.0	123.50
∠ HC(2)C(1)	122.92	122.87	123.2	123.05

^a C(1)–H and C(2)–H, ∠ HC(1)C(2) and ∠ HC(2)C(1) assumed equal.^b RHF/6-31G* calculation, C(1)–H and C(2)–H assumed equal.

Throughout the present work all valence electrons have been correlated in CCSD(T) and MP4 calculations, carried out using the MOLPRO suite of programs.^{7,13}

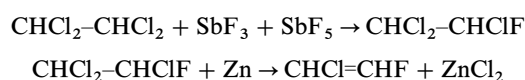
2.2 Results and discussion

The equilibrium geometries of *cis*-1-chloro-2-fluoroethylene, obtained using CCSD(T) and MP4 with cc-pVTZ basis, are reported in Table 1. First of all, we can note that both *ab initio* methods yield nearly indistinguishable results, in fact the maximum difference is 0.003 Å for bond lengths and less than 0.1° for angles. In general CCSD(T) calculations give very reliable results for equilibrium geometry determination^{14,15} and, usually, the errors are very systematic, *i.e.* CCSD(T) tends to overestimate the bond distances. According to the vast literature on this topic (see for example refs. 14–17), we can assume an accuracy of 0.002–0.006 Å for bond lengths and 0.1–0.5° for angles. Unfortunately, no experimental values are presently available to compare our results; we can only make comparisons with a recent, but not of high quality, *ab initio* computation¹⁸ and an empirical structure presented in an old microwave investigation.¹ In ref. 1 an assumed structure based on the geometries of vinyl chloride and vinyl fluoride was used since the agreement between the moments of inertia calculated from this structure and the corresponding observed values suggested that the empirical geometry was approximately correct. As we can see in Table 1, an overall agreement of this assumed structure with our computed geometry has been found. On the other hand, worse results are presented in ref. 18, in which all bond lengths and bond angles are underestimated and overestimated, respectively; in particular the C–C and C–F bond distances are too short.

3 Molecular dipole moment

3.1 Experimental details

3.1.1 Synthesis of 1-chloro-2-fluoroethylene. The route to synthesize CHCl=CHF is represented by the following reactions:



In a Pyrex glass apparatus, CHCl₂–CHCl₂ (99%, Aldrich) was fluorinated with SbF₃ (99.8%, Aldrich) using SbF₅ (54%, Aldrich) as activating reactant. This method, proposed by Kolesnikov and Avetyan¹⁹ has the great advantage that it can be carried out in glass apparatus and the reactions take place at atmospheric pressure.²⁰

The reaction mixture was heated at 130–135 °C for 6 h while the products continuously distilled out. Crude monofluorinated product, bp 101–105 °C, was rectified through a Dafton column and the resulting CHCl₂–CHClF boiled at 102–103 °C (literature value:²¹ 102.2–102.6 °C). The survey

infrared spectrum for CHCl₂–CHClF in CS₂ solution was recorded with a low-resolution FTIR spectrometer and the principal absorption bands with approximate intensities are: 3000(m), 2980(m), 1204(m), 1113(vs), 1084(s), 1066(s), 1039(s), 1026(s), 960(m), 825(s), 794(vs), 752(vs), 743(vs), 666(m), 615(m) and 567(m) cm^{−1}. These data, not available in the literature, are given for a comprehensive report on the experiment.

By 1,2-elimination reaction, CHCl₂–CHClF was dechlorinated reacting with zinc in refluxing ethanol to afford a *cis*–*trans* mixture of CHCl=CHF which was condensed into a cryogenic trap cooled at dry ice temperature.²²

The specimen of the diastereoisomer *cis*-CHCl=CHF was recovered from the *Z*–*E* mixture by trap-to-trap condensation at low temperature under dynamic vacuum, employing a slush bath of 2-methylbutane and liquid nitrogen (temperature ranges from −115 to −95 °C). The purity of *cis*-CHCl=CHF was tested by gas-phase low-resolution infrared spectroscopy.³

3.1.2 Measurements of the Stark spectra. The Stark spectrum of *cis*-1-chloro-2-fluoroethylene has been observed in the region 12–18 GHz using a conventional P band wave guide Stark cell 1.5 m long. This cell has been calibrated by measuring the Stark shifts of the *J* = 1 ← 0 transition of OCS at several values of the applied electric field ($\mu_{\text{OCS}} = 0.71521(20)$ D).²³

The spectra have been recorded at dry ice temperature and within a pressure range of 1–3 mbar. The Stark field has been obtained by applying to the cell electrodes a zero based square wave modulated high voltage signal from a power supply working at a frequency of 10 kHz.

The microwave source is a computer controlled HP frequency synthesiser (12–18 GHz) which is phase synchronised to a 10 MHz reference signal from a Rubidium standard. The computer, while driving the radiation source, collects data at each frequency step from a lock-in amplifier tuned at the frequency of the applied electric field; processing of the spectra, such as averaging and background subtraction, may be easily performed. A more detailed description of the spectrometer and technique used are described elsewhere.²⁴

3.2 Rotational–quadrupole–Stark Hamiltonian

The total rotational Hamiltonian for an asymmetric top molecule with one quadrupolar nucleus in a static electric field can be written as a sum of the asymmetric rotor, the quadrupole coupling and the Stark interaction terms:

$$H_{\text{rot}} = H_{\text{asym}} + H_Q + H_{\text{Stark}} \quad (1)$$

Using the symmetric top wave functions $|KJIFM_F\rangle$ in the coupled representation as basis set, for the *A*-reduced Hamiltonian in the *I'* representation the matrix elements are diagonal in the rotational quantum number *J* and assume the following form:

$$\begin{aligned} \langle KJ | H_{\text{asym}} | KJ \rangle &= \frac{1}{2}(B + C)J(J + 1) + [A - \frac{1}{2}(B + C)]K^2 \\ &\quad - \Delta_J J^2(J + 1)^2 - \Delta_{JK} J(J + 1)K^2 - \Delta_K K^4 \\ &\quad + \Phi_J J^3(J + 1)^3 + \Phi_{JK} J^2(J + 1)^2 K^2 \\ &\quad + \Phi_{KJ} J(J + 1)K^4 + \Phi_K K^6, \end{aligned} \quad (2)$$

$$\begin{aligned} \langle K \pm 2J | H_{\text{asym}} | KJ \rangle &= \left\{ \frac{1}{4}(B - C) - \delta_J J(J + 1) \right. \\ &\quad \left. - \frac{1}{2}\delta_K [(K \pm 2)^2 + K^2] + \phi_J J^2(J + 1)^2 \right. \\ &\quad \left. + \frac{1}{2}\phi_{JK} J(J + 1)[(K \pm 2)^2 + K^2] \right. \\ &\quad \left. + \frac{1}{2}\phi_K [(K \pm 2)^4 + K^4] \right\} \\ &\quad \times \{ [J(J + 1) - K(K \pm 1)][J(J + 1) \\ &\quad - (K \pm 1)(K \pm 2)] \}^{1/2}. \end{aligned} \quad (3)$$

The quadrupole Hamiltonian connects states with *J* differing by 0, ±1 and ±2, and, for a molecule lying in the *ab*

plane, its matrix elements, nonzero for $\Delta K = 0, \pm 1, \pm 2$, are given by:

$$\begin{aligned} \langle K'J'IF_M_F | H_Q | KJIF_M_F \rangle = & (-1)^{J+I+F} \left[2 \begin{pmatrix} I & 2 & I \\ I & 0 & -I \end{pmatrix} \right]^{-1} \\ & \times \left\{ \begin{matrix} F & I & J' \\ 2 & J & I \end{matrix} \right\} \sqrt{(2J+1)(2J'+1)} \frac{1}{2} \\ & \times \left[(-1)^{J-K} \begin{pmatrix} J & 2 & J' \\ K & 0 & -K' \end{pmatrix} \right. \\ & \times \chi_{aa} \mp (-1)^{J-K \mp 1} \begin{pmatrix} J & 2 & J' \\ K & \pm 1 & -K' \end{pmatrix} \\ & \times \sqrt{\frac{2}{3}} \chi_{ab} + (-1)^{J-K \mp 2} \\ & \left. \times \begin{pmatrix} J & 2 & J' \\ K & \pm 2 & -K' \end{pmatrix} \frac{1}{\sqrt{6}} (\chi_{bb} - \chi_{cc}) \right], \quad (4) \end{aligned}$$

where the usual notation for $3-j$ symbols and $6-j$ symbols is adopted. Finally, the elements of the Stark Hamiltonian matrix are nonzero for $\Delta J = 0, \pm 1$, $\Delta F = 0, \pm 1$ and $\Delta M_F = 0$, with terms in μ_a connecting states with $\Delta K = 0$, and those in μ_b with $\Delta K = \pm 1$:

$$\begin{aligned} \langle K'J'IF'_M_F | H_{\text{Stark}} | KJIF_M_F \rangle = & -\mathcal{E}(-1)^{F'-M_F} \begin{pmatrix} F' & 1 & F \\ -M_F & 0 & M_F \end{pmatrix} \\ & \times (-1)^{J'+I+F+1} \sqrt{(2F+1)(2F'+1)} \\ & \times \left\{ \begin{matrix} J' & F' & I \\ F & J & I \end{matrix} \right\} (-1)^{J'-K} \sqrt{(2J+1)(2J'+1)} \\ & \times \left\{ \begin{pmatrix} J' & J & 1 \\ K' & -K & 0 \end{pmatrix} \mu_a + \left[\begin{pmatrix} J' & J & 1 \\ K' & -K & -1 \end{pmatrix} \right. \right. \\ & \left. \left. - \begin{pmatrix} J' & J & 1 \\ K' & -K & +1 \end{pmatrix} \right] \frac{1}{\sqrt{2}} \mu_b \right\}, \quad (5) \end{aligned}$$

where \mathcal{E} is the value of the applied electric field, which is in our case parallel to the electric radiation field.

The only “good” quantum number is M_F , and for each of its values the Hamiltonian matrix has to be set up with proper truncation in F , that is $\Delta F = +2$, as upper bound and $\Delta F = -2$, as lower bound, above and below the F values of the transition of interest, respectively. However, direct diagonalization of such a matrix does not allow assignment of “nearly good” quantum numbers F, J, K_a and K_c to eigenvalues, thus the procedure listed in the following items has been devised: (i) input values for: F_{\min}, F_{\max} and M_F , spectroscopic constants and quadrupole tensor,^{1,2} dipole moment, Stark field; (ii) build H_{asym} matrix, transform into Wang basis, diagonalize, assign eigenvalues; (iii) build H_Q matrix and H_{Stark} matrix, sum the matrices; (iv) transform into asymmetric basis, add asymmetric top eigenvalues; (v) diagonalize, assign eigenvalues by a projection technique;²⁵ and (vi) transform dipole moment matrices into final basis to compute line strengths.

The final step is intended for determining the relative intensity of the hyperfine-Stark components, whose transition frequencies may be computed by the difference of the energy levels J_{K_a, K_c}, F', M_F and J_{K_a, K_c}, F, M_F with $\Delta F = 0, \pm 1$.

3.3 Results and discussion

In order to measure the dipole moment of *cis*-1-chloro-2-fluoroethylene, we have observed the Stark effect for the two

rotational transitions $4_{0,4} \leftarrow 3_{1,3}$ and $4_{1,3} \leftarrow 4_{0,4}$, chosen for the following reasons:

(i) The absorption coefficients α_{\max} of these two transitions are large enough to ensure a good signal-to-noise ratio of the spectra.

(ii) For the $4_{1,3} \leftarrow 4_{0,4}$ transition, the shifts of the Stark components are mainly due to the μ_b component of the dipole moment, while for the $4_{0,4} \leftarrow 3_{1,3}$ the μ_a component gives the stronger contributions. Thus, by observing the Stark spectra of both of them, a quite accurate value of the dipole moment of *cis*-1-chloro-2-fluoroethylene can be determined.

(iii) The frequency regions, where these two transitions fall, are free from other interfering transitions which could make the line profiles analysis more complicate.

As previously mentioned, the lock-in amplifier is tuned at the same frequency of the applied electric field so that the zero field lines are 180° out of phase compared to the Stark components, as can be seen in Fig. 1. It is also evident that the strongest components of the quadrupole hyperfine structure, due to the chlorine nucleus ($I = 3/2$), are well resolved at zero field while the Stark components do not present a resolved hyperfine structure. In fact the inhomogeneity of the applied electric field, resulting from the imperfect geometry of the Stark cell, produces a broadening of the Stark components which becomes larger as the Stark shift grows. From such premises it proceeds that each resolved Stark component in the experimental spectra is in fact the overlapping of several hyperfine components that are frequency shifted by the applied electric field.

By using the computer program described in the previous paragraph and the *ab initio* predicted values of μ_a and μ_b (see later on), for each value of the applied electric field it has been possible to obtain calculated spectra as a sum of a number of Lorentzian functions, corresponding to all the possible predicted components. Then, these calculated spectra have been compared with those experimentally observed and optimised using a least squares fitting procedure.

The data of the iteration procedure are the differences, point by point, between observed and calculated spectra. The adjustable parameters, determined following the least squares criteria of best fit, are: (i) One scale factor I_s , the same for each resolved Stark component of the observed spectrum. This factor adjusts the calculated intensity to the observed one. (ii) The Lorentzian halfwidths γ_s , the same for all the hyperfine components of a given experimentally resolved Stark component. (iii) The two components μ_a and μ_b of the dipole moment.

In practice, the model used to minimize the differences between observed (S_i^{obs}) and calculated (S_i^{calc}) spectra is the following:

$$\begin{aligned} S_i^{\text{obs}} - S_i^{\text{calc}} = & \sum_s \sum_n L_{i,n,s} \Delta I_s \\ & + \sum_s I_s \sum_n \frac{\partial L_{i,n,s}}{\partial v_{0n}} \frac{\partial v_{0n}}{\partial \mu_a} \Delta \mu_a \\ & + \sum_s I_s \sum_n \frac{\partial L_{i,n,s}}{\partial v_{0n}} \frac{\partial v_{0n}}{\partial \mu_b} \Delta \mu_b \\ & + \sum_s I_s \sum_n \frac{\partial L_{i,n,s}}{\partial \gamma_s} \Delta \gamma_s, \quad (6) \end{aligned}$$

where the Lorentzian function $L_{i,n,s}$ is given by

$$L_{i,n,s} = I_n \frac{\gamma_s}{\gamma_s^2 + (v_i - v_{0n})^2}. \quad (7)$$

I_n and v_{0n} are the calculated intensity of the n -th hyperfine component and the Lorentzian central frequency, respectively. The label s runs over the experimentally resolved Stark components, n over the unresolved hyperfine components, within

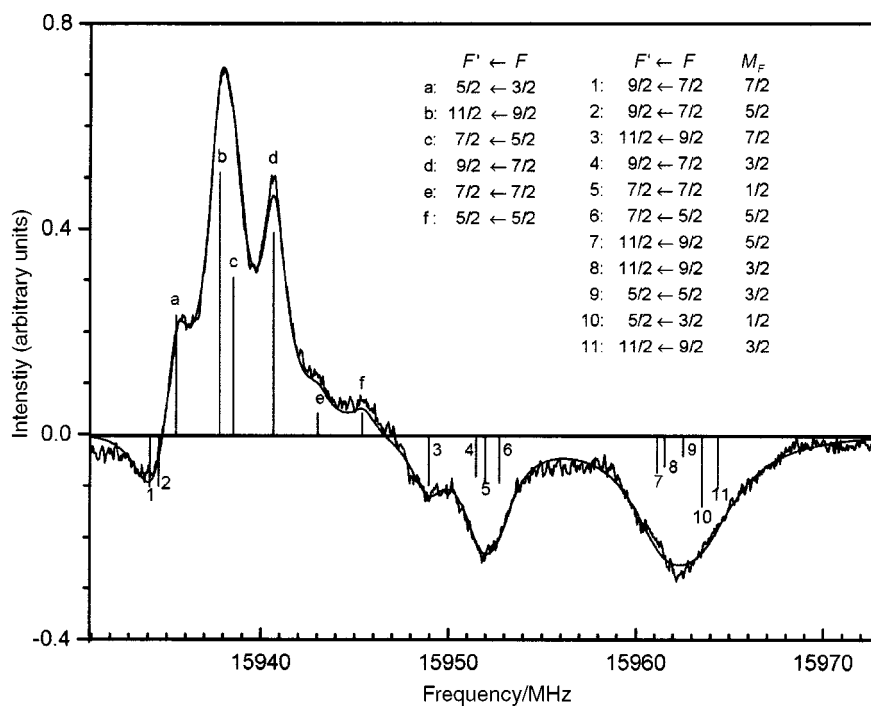


Fig. 1 Stark spectrum of the $4_{0,4} \leftarrow 3_{1,3}$ rotational transition of *cis*-1-chloro-2-fluoroethylene with an applied electric field of 1916 V cm^{-1} . The experimental and calculated line profiles are presented along with a stick spectrum showing the positions of the blended hyperfine-Stark components.

each experimentally resolved Stark component and i specifies the i -th point of the spectrum.

While the derivatives of the Lorentzian function with respect to ν_0 and γ_s have been obtained analytically, the derivatives of ν_0 with respect to μ_a and μ_b have been determined numerically.

The final values of μ_a (0.633(3) D) and μ_b (2.072(1) D) have been obtained by analysing simultaneously 8 experimental Stark spectra of the $4_{0,4} \leftarrow 3_{1,3}$ and $4_{1,3} \leftarrow 4_{0,4}$ transitions. An example of these spectra is reported in Fig. 1, where the observed and calculated spectra are shown along with the stick spectrum obtained using the final values of μ_a and μ_b .

No previous experimental values are known; only a preliminary treatment of the Stark effect of the $1_{11} \leftarrow 0_{00}$ multiplet was reported by Howe,¹ who proposed a value of 1.6 D for the b component of the dipole moment. In general, Howe assumed that μ_b should be estimated at 1 to 2 D, but the presence of quadrupole coupling prevented a more detailed analysis.

As mentioned in the previous section, in the theoretical evaluation of the equilibrium dipole moment both CCSD(T) and MP4 calculations have been performed, employing the cc-pVTZ basis set. Being both CCSD(T) and MP4 post-Hartree-Fock methods, the dipole moment has been estimated numerically as energy derivative, *i.e.*, first derivative of the total energy with respect to a homogeneous electric field at zero field strength.

As is evident in ref. 26, inclusion of diffuse functions in the basis set is important for an accurate evaluation of the molecular dipole moment. Since the CCSD(T)/aug-cc-pVTZ (234 cGTOs) calculation²⁷ proved too big for our workstations and since the diffuse orbitals are particularly useful to correctly describe the electronegative atoms, *i.e.* F and Cl, we decided to also perform the computation at CCSD(T) level using the (aug)-cc-pVTZ basis set (184 cGTOs), where (aug) means that we have employed the aug-cc-pVTZ for F and Cl atoms, but the cc-pVTZ basis for C and H.

The computed μ_a and μ_b components—where a and b denote the principal axes of inertia, depicted in Fig. 2—and total dipole moment are listed and compared to experiment in

Table 2. In this table the total dipole moment evaluated is also reported in a semiempirical MNDO calculation by Dewar and Rzepa,²⁸ and appears overestimated by more than 10%.

In Table 2 we can see a very good agreement between calculated and experimental values, from which an accuracy of about 0.05 D for our computations can be deduced. These results were not improved by using the (aug)-cc-pVTZ basis, in fact we obtained for μ_a a very similar value (0.67 D), while μ_b was overestimated by nearly 0.05 D, instead of being underestimated by the same quantity. Maybe better results could be reached employing the aug-cc-pVTZ basis set for all atoms, as the (aug)-cc-pVTZ probably does not give a balanced description. In order to fill this gap, we have evaluated the two-point extrapolated basis set limit using both the cc-pVXZ ($X = \text{D, T}$) and (aug)-cc-pVXZ ($X = \text{D, T}$) basis sets. For the cc-pVXZ bases, the extrapolated values of μ_a and μ_b are only a little better (~ 0.01 D) than the unextrapolated results, while the extrapolation employing the (aug)-cc-pVXZ basis sets gives improved predictions, with perfect agreement to the experiment, as can be seen in Table 2.

Finally, as previously seen for the equilibrium geometry, CCSD(T) and MP4 methods give similar results, in fact the maximum difference is only 0.004 D for μ_b ; in particular, we notice that both methods slightly overestimate μ_a and underestimate μ_b using cc-pVTZ basis, while overestimating them both with (aug)-cc-pVTZ. As expected, since the coupled cluster approach is able to treat non-dynamical correlation

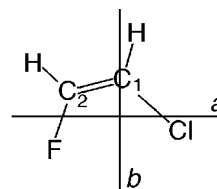


Fig. 2 *Cis*-1-chloro-2-fluoroethylene molecule: orientation of the a and b principal inertial axes, lying in the molecular plane; the c axis is perpendicular to that plane.

Table 2 Comparison between computed and experimental μ_a , μ_b and total dipole moment (D) of *cis*-1-chloro-2-fluoroethylene

	MP4/VTZ	CCSD(T)/VTZ	Extrapolated ^a	Ref. 28 ^b	Exp. ^c
μ_a	0.68	0.69	0.648	—	0.633(3)
μ_b	1.98	2.02	2.071	—	2.072(1)
μ_{tot}	2.10	2.13	2.17	2.45	(2.167)

^a (aug)-cc-pVXZ (X = D, T) basis sets (see text). ^b MNDO semiempirical calculation. ^c This work.

better than finite-order perturbation theory (see for example ref. 29), the nearest value to experiment has been obtained with CCSD(T) calculation.

4 Conclusions

The electric dipole moment of *cis*-1-chloro-2-fluoroethylene, which up to now was unknown, has been determined from the simultaneous analysis of 8 experimental Stark spectra of the $4_{0,4} \leftarrow 3_{1,3}$ and $4_{1,3} \leftarrow 4_{0,4}$ rotational transitions. This result was achieved with the help of high quality *ab initio* calculations which also gave accurate predictions of the equilibrium geometry. The experimental and theoretical procedures set out in this work will be useful in extending these investigations to other halogenated compounds having one chlorine nucleus.

Acknowledgements

This work has been supported by the Ministero dell'Università e della Ricerca Scientifica e Tecnologica (MURST 40%), by CNR, by the University of Bologna (funds for selected research topics and ex-60%) and by the European Union under Contract No. ERBFMRXCT960088. The authors would like to thank the referees for useful suggestions concerning accurate calculations of the molecular dipole moment.

References

- 1 J. A. Howe, *J. Chem. Phys.*, 1961, **34**, 1247.
- 2 J. L. Alonso, A. G. Lesarri, L. A. Leal and J. C. López, *J. Mol. Spectrosc.*, 1993, **162**, 4.
- 3 N. C. Craig, Y.-S. Lo, L. G. Piper and J. C. Wheeler, *J. Phys. Chem.*, 1970, **74**, 1712.
- 4 R. Atkinson and W. P. L. Carter, *Chem. Rev.*, 1984, **84**, 437.
- 5 R. Atkinson, *Chem. Rev.*, 1986, **86**, 69.
- 6 P. Stoppa, S. Giorgianni, R. Visinoni and S. Ghersesti, *Mol. Phys.*, 1999, **97**, 329.
- 7 C. Hampel, K. Peterson and H.-J. Werner, *Chem. Phys. Lett.*, 1992, **190**, 1.
- 8 K. Raghavachari, G. W. Trucks, J. A. Pople and M. Head-Gordon, *Chem. Phys. Lett.*, 1989, **156**, 479.
- 9 M. J. O. Deegan and P. J. Knowles, *Chem. Phys. Lett.*, 1994, **227**, 321.
- 10 C. Møller and M. S. Plesset, *Phys. Rev.*, 1934, **46**, 618.
- 11 T. H. Dunning, Jr., *J. Chem. Phys.*, 1989, **90**, 1007.
- 12 T. Helgaker, J. Gauss, P. Jørgensen and J. Olsen, *J. Chem. Phys.*, 1997, **106**, 6430.
- 13 MOLPRO is a package of *ab initio* programs written by H.-J. Werner and P. J. Knowles, with contributions of J. Almlöf, R. D. Amos, M. J. O. Deegan, S. T. Ebert, C. Hampel, W. Meyer, K. Peterson, R. M. Pitzer, A. J. Stone and P. R. Taylor.
- 14 H. F. Schaefer III, J. R. Thomas, Y. Yamaguchi, B. J. DeLeeuw and G. Vacek, in *Modern Electronic Structure Theory—Part I*, ed. D. R. Yarkony, World Scientific, Singapore, 1995, pp. 3–54. Advances Series in Physical Chemistry, vol. II.
- 15 P. Botschwina, M. Oswald, J. Flügge, Ä. Heyl and R. Oswald, *Chem. Phys. Lett.*, 1993, **209**, 117.
- 16 P. Botschwina, M. Horn, K. Markey and R. Oswald, *Mol. Phys.*, 1997, **92**, 381.
- 17 P. Botschwina, Ä. Heyl, W. Chen, M. C. McCarthy, J.-U. Grabow, M. J. Travers and P. Thaddeus, *J. Chem. Phys.*, 1998, **109**, 3108.
- 18 V. P. Feshin and M. Yu. Konshin, *J. Struct. Chem.*, 1998, **39**, 128.
- 19 G. S. Kolesnikov and M. G. Avetyan, *Izv. Akad. Nauk SSSR, Otd. Khim. Nauk*, 1959, 331; G. S. Kolesnikov and M. G. Avetyan, *Chem. Abstr.*, 1959, **53**, 19942a.
- 20 M. Hudlicky, *Chemistry of Organic Fluorine Compounds*, Ellis Horwood Ltd., Chichester, UK, 2nd edn., 1992, p. 101.
- 21 M. Hauptschein and L. A. Bigelow, *J. Am. Chem. Soc.*, 1951, **73**, 5591.
- 22 H. G. Viehe, *Ber. Dtsch. Chem. Ges.*, 1960, **93**, 1697.
- 23 J. S. Muentner, *J. Chem. Phys.*, 1968, **48**, 4544.
- 24 L. Dore, L. Cludi, A. Mazzavillani, G. Cazzoli and C. Puzzarini, *Phys. Chem. Chem. Phys.*, 1999, **1**, 2275.
- 25 H. M. Pickett, *J. Mol. Spectrosc.*, 1991, **148**, 371.
- 26 A. Halkier, W. Klopper, T. Helgaker and P. Jørgensen, *J. Chem. Phys.*, 1999, **111**, 4424.
- 27 R. A. Kendall, T. H. Dunning, Jr. and R. J. Harrison, *J. Chem. Phys.*, 1992, **96**, 6796.
- 28 M. J. S. Dewar and H. S. Rzepa, *J. Comput. Chem.*, 1983, **4**, 158.
- 29 G. E. Scuseria and T. J. Lee, *J. Chem. Phys.*, 1990, **93**, 5851.

Paper a910297n